



HAL
open science

Endoplasmic reticulum stress induces inverse regulations of major functions in portal myofibroblasts during liver fibrosis progression

Emilien Loeuillard, Haquima El Mourabit, Lin Lei, Sara Lemoinne, Chantal Housset, Axelle Cadoret

► To cite this version:

Emilien Loeuillard, Haquima El Mourabit, Lin Lei, Sara Lemoinne, Chantal Housset, et al.. Endoplasmic reticulum stress induces inverse regulations of major functions in portal myofibroblasts during liver fibrosis progression. *Biochimica et Biophysica Acta - Molecular Basis of Disease*, 2018, 1864 (12), pp.3688-3696. 10.1016/j.bbadis.2018.10.008 . hal-03971660

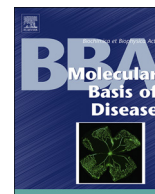
HAL Id: hal-03971660

<https://hal.sorbonne-universite.fr/hal-03971660>

Submitted on 3 Feb 2023

HAL is a multi-disciplinary open access archive for the deposit and dissemination of scientific research documents, whether they are published or not. The documents may come from teaching and research institutions in France or abroad, or from public or private research centers.

L'archive ouverte pluridisciplinaire **HAL**, est destinée au dépôt et à la diffusion de documents scientifiques de niveau recherche, publiés ou non, émanant des établissements d'enseignement et de recherche français ou étrangers, des laboratoires publics ou privés.



Endoplasmic reticulum stress induces inverse regulations of major functions in portal myofibroblasts during liver fibrosis progression



Emilien Loeuillard^{a,1}, Haquima El Mourabit^a, Lin Lei^a, Sara Lemoine^{a,b}, Chantal Housset^{a,b,*}, Axelle Cadoret^a

^a Sorbonne Université, INSERM, Saint-Antoine Research Center (CRSA), Institute of Cardiometabolism and Nutrition (ICAN), Paris, France

^b Assistance Publique-Hôpitaux de Paris, Hôpital Saint-Antoine, Hepatology Department, Reference Center for Inflammatory Biliary Diseases and Autoimmune Hepatitis, Paris, France

ARTICLE INFO

Keywords:

Liver fibrosis
Angiogenesis
Bile duct ligation
PKR-like endoplasmic reticulum kinase (PERK)
Unfolded protein response (UPR)

ABSTRACT

Portal myofibroblasts (PMF) form a sub-population of highly proliferative and proangiogenic liver myofibroblasts that derive from portal mesenchymal progenitors. Endoplasmic reticulum (ER) stress was previously shown to modulate fibrogenesis, notably in the liver. Our aim was to determine if ER stress occurred in PMF and affected their functions. PMF were obtained after their expansion *in vivo* from bile duct-ligated (BDL) rats and referred to as BDL PMF. Compared to standard PMF obtained from normal rats, BDL PMF were more myofibroblastic, as assessed by higher alpha-smooth muscle actin expression and collagen 1 production. Their proangiogenic properties were also higher, whereas their proliferative and migratory capacities were lower. CHOP expression was detected in the liver of BDL rats, at the leading edge of portal fibrosis where PMF accumulate. BDL PMF displayed ER dilatation and an overexpression of the PERK pathway downstream targets, *Chop*, *Gadd34* and *Trb3*, in comparison with standard PMF. *In vitro*, the induction of ER stress by tunicamycin in standard PMF, caused a decrease in their proliferative and migratory activity, and an increase in their proangiogenic activity, without affecting their myofibroblastic differentiation. Conversely, the treatment of BDL PMF with the PERK inhibitor GSK2656157 reduced ER stress, which caused a decrease in their angiogenic properties, and restored their proliferative and migratory capacity. In conclusion, PMF develop ER stress as they expand with the progression of fibrosis, which further increases their proangiogenic activity, but also inhibits their proliferation and migration. This phenotypic switch may restrict PMF expansion while they support angiogenesis.

1. Introduction

Myofibroblasts are matrix-producing cells that arise in fibrotic diseases. They have different possible origins and serve a wide range of functions related to wound healing. Alpha-smooth muscle actin (α -SMA) is their most commonly used marker [1]. In the liver, hepatic stellate cells (HSC) are the major but not exclusive source of myofibroblasts [2]. Portal myofibroblasts (PMF) form a distinct population of

liver myofibroblasts that derive from portal mesenchymal cells [3–7]. While PMF contribute to the progression of liver fibrosis in all types of liver diseases [8], they are the major population of myofibroblasts that accumulate at early stages of cholestatic liver injury [3,4,6,9,10]. We previously showed that PMF were highly proliferative, as opposed to HSC-derived myofibroblasts [11]. We also showed that they were key cells in angiogenesis, a mechanism which drives the progression of liver fibrosis from portal tracts into the parenchyma [8,12].

Abbreviations: α -SMA, alpha-smooth muscle actin; ATF6, activating transcription factor 6; BDL, bile duct ligation; BSA, bovine serum albumin; CHOP, CCAAT-enhancer-binding protein homologous protein; CM, conditioned medium; COL1a1, collagen, type 1, alpha 1; DMSO, dimethyl sulfoxide; ER, endoplasmic reticulum; FBS, fetal bovine serum; FGF2, fibroblast growth factor-2; GADD34, growth arrest and DNA damage-inducible protein 34; HPRT, hypoxanthine phosphoribosyl transferase; HSC, hepatic stellate cell; IRE1, inositol-requiring enzyme 1; MCP-1, monocyte chemoattractant protein-1; NAFLD, non-alcoholic fatty liver disease; PDGF-BB, platelet-derived growth factor-BB; PERK, PKR-like endoplasmic reticulum kinase; PMF, portal myofibroblast; RT-qPCR, Reverse transcription-quantitative polymerase chain reaction; TM, tunicamycin; UPR, unfolded protein response; VEGF, vascular endothelial growth factor; vWF, von Willebrand factor

* Corresponding author at: Faculté de Médecine Sorbonne Université, Site Saint-Antoine, 27 rue Chaligny, 75571 Paris cedex 12, France.

E-mail addresses: loeuillard.emilien@mayo.edu (E. Loeuillard), haquima.el-mourabit@inserm.fr (H. El Mourabit), lin.lei@inserm.fr (L. Lei), chantal.housset@inserm.fr (C. Housset), axelle.cadoret@inserm.fr (A. Cadoret).

¹ Present address: Division of Gastroenterology and Hepatology, Mayo Clinic, Rochester, Minnesota 55905, USA.

<https://doi.org/10.1016/j.bbadis.2018.10.008>

Received 22 June 2018; Received in revised form 27 September 2018; Accepted 2 October 2018

Available online 04 October 2018

0925-4439/ © 2018 Elsevier B.V. All rights reserved.

Mounting evidence indicates that endoplasmic reticulum (ER) stress is associated with the development and progression of fibrotic diseases [13–16]. Under stress conditions, the ER initiates the unfolded protein response (UPR) to restore homeostasis. The UPR is mediated by three ER transmembrane sensors: the inositol-requiring enzyme 1 (IRE1), the activating transcription factor 6 (ATF6) and the PERK-like endoplasmic reticulum kinase (PERK). Each pathway culminates to promote the expression of genes required to reestablish ER homeostasis, through i) translational attenuation of global protein synthesis and ii) protein degradation. The PERK pathway plays a major role in reducing translation rates via the phosphorylation of eIF2 α . Phosphorylated eIF2 α also promotes the preferential translation of the transcription factor ATF4, which in turn induces the up-regulation of CCAAT-enhancer-binding protein homologous protein (CHOP) and growth arrest and DNA damage-inducible protein 34 (GADD34) genes. Ultimately, this response allows to counteract stress or direct cell fate towards apoptosis. When UPR fails to adapt, ER stress triggers a pathological response.

Previous work provided evidence to indicate that ER stress can occur in HSC and thereby promote liver fibrosis. Thus, it was shown in mouse models of liver fibrosis caused by ethanol or carbon tetrachloride, that ER stress developed in HSC and triggered their fibrogenic activity [15,17]. Blockade of the IRE1 pathway decreased HSC fibrogenic activity [17], whereas the chemical induction of ER stress, by tunicamycin (TM) or thapsigargin in HSC, caused an up-regulation of fibrogenic genes [15,18]. On the other hand, ER stress could also promote HSC apoptosis and thereby contribute to the resolution of fibrosis. Thus, cannabidiol was shown to cause the death of myofibroblastic HSC by a mechanism of ER stress-induced apoptosis [19]. It has also been possible to trigger ER stress-induced apoptosis and thereby reduce collagen synthesis, by overexpressing the matricellular protein CCN1 in HSC [20].

As compared with HSC-derived myofibroblasts, PMF display a number of distinct phenotypic features [8,21]. They also accumulate with a different spatial and temporal pattern during the progression of liver fibrosis [6,7]. While the mechanisms regulating the phenotypic changes of HSC during fibrogenesis have been largely unraveled [2], those underlying the phenotypic changes of PMF are still poorly known. In the present study, we investigated PMF phenotype following their expansion *in vivo*, with particular attention to ER stress. We determined if PMF developed ER stress as they accumulated in the fibrotic liver and if this impacted their functions.

2. Materials and methods

2.1. Animals

Male Sprague Dawley rats weighing 200–250 g were purchased from Janvier Labs, Le Genest-Saint-Isle, France. Bile duct ligation (BDL) and sham operation were performed as previously described [4]. All procedures were approved by the Charles Darwin Ethical Committee for Animal Studies (Approval N°01163 01), and by the Institutional Animal Care and Use Department (DSV, Paris, Agreement N°75-12-01).

2.2. Cell models

PMF were obtained from normal or 2-week BDL rats, following an established protocol [11] and were referred to as standard and BDL PMF, respectively. Standard and BDL PMF were first compared in primary culture (P0). Subsequently, standard PMF were equally used at P0 or after one passage (P1), as their phenotype at P0 and P1 was previously shown to be the same [11]. When indicated, PMF were incubated with 1 μ mol/L of TM (Merck, Fontenay sous Bois, France) to induce ER stress or with 1 μ mol/L of the PERK inhibitor GSK2656157 (Merck, Darmstadt, Germany), for 24 h. Control cells were incubated with vehicle, *i.e.* dimethyl sulfoxide (DMSO, 1/1000). Conditioned

media (CM) were obtained from PMF incubated with serum-free or 10% fetal bovine serum (FBS)-containing medium, for 24 h.

2.3. (Immuno)staining

Paraffin-embedded formalin-fixed 4- μ m-thick liver tissue sections were subjected to Sirius red staining or immunostaining, using anti- α -SMA (#M0851; Dako, Les Ulis, France), anti-von Willebrand factor (vWF) (#GTx60934; Clinisciences, Nanterre, France) or anti-CHOP (#ab11419; Abcam, Paris, France), as primary antibodies, horseradish peroxidase-conjugated antibodies (Vector laboratories, Peterborough, UK), as secondary antibodies and 3-amino-9-ethylcarbazole (Vector laboratories) as a substrate. Tissue sections were counterstained with Mayer's hematoxylin. For immunofluorescence, cell preparations were fixed in 4% paraformaldehyde and incubated with primary antibodies against Calreticulin (#sc11398; Santa Cruz Biotechnology, Dallas, TX, USA) or α -SMA (#M0851; Dako). Nuclear staining was performed using Draq5 (Ozyme, Saint-Quentin-en-Yvelines, France). Cells were examined with a SP2 confocal microscope (Leica, Bannockburn, IL, USA).

2.4. Transmission electron microscopy

Cells were fixed with 2% glutaraldehyde in 0.1 mol/L sodium cacodylate buffer (pH 7.4) for 30 min at 4 °C and post-fixed with 1% osmium tetroxide in the same buffer for 30 min at 4 °C. Samples were then dehydrated and embedded in epoxy resin. Ultra-thin (60 nm) sections were contrast-enhanced using uranyl acetate and lead citrate and examined using a JEOL 1010 electron microscope with a MegaView III camera.

2.5. Reverse transcription-quantitative polymerase chain reaction (RT-qPCR)

The cDNA obtained from total RNA was subjected to quantitative real-time PCR using the Sybr Green Master Mix (Roche Diagnostics, Meylan, France) on a Lightcycler 96 device (Roche Diagnostics). Primer sequences are provided in Supplementary Table 1. Target gene mRNA levels are reported relative to a calibrator according to the $2^{-\Delta\Delta CT}$ method, using hypoxanthine phosphoribosyl transferase (HPRT) as a reference gene, the expression of which was stable in ER stress condition.

2.6. Immunoblotting

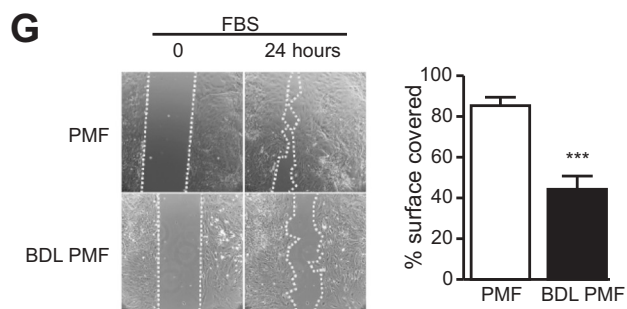
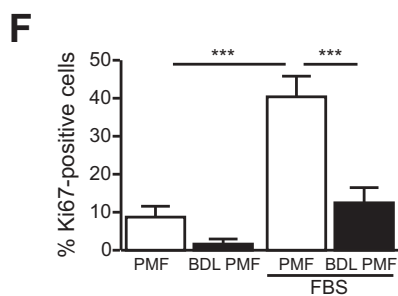
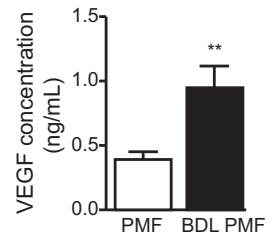
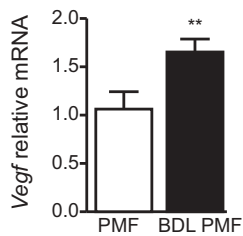
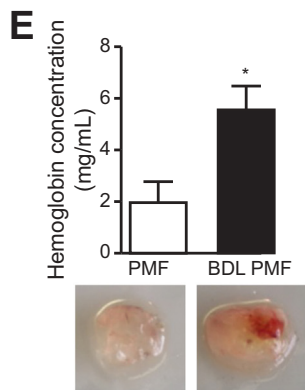
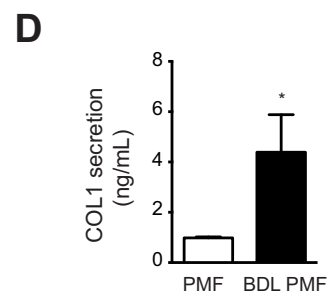
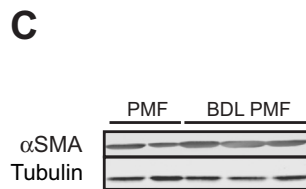
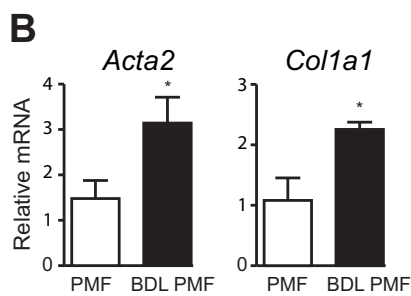
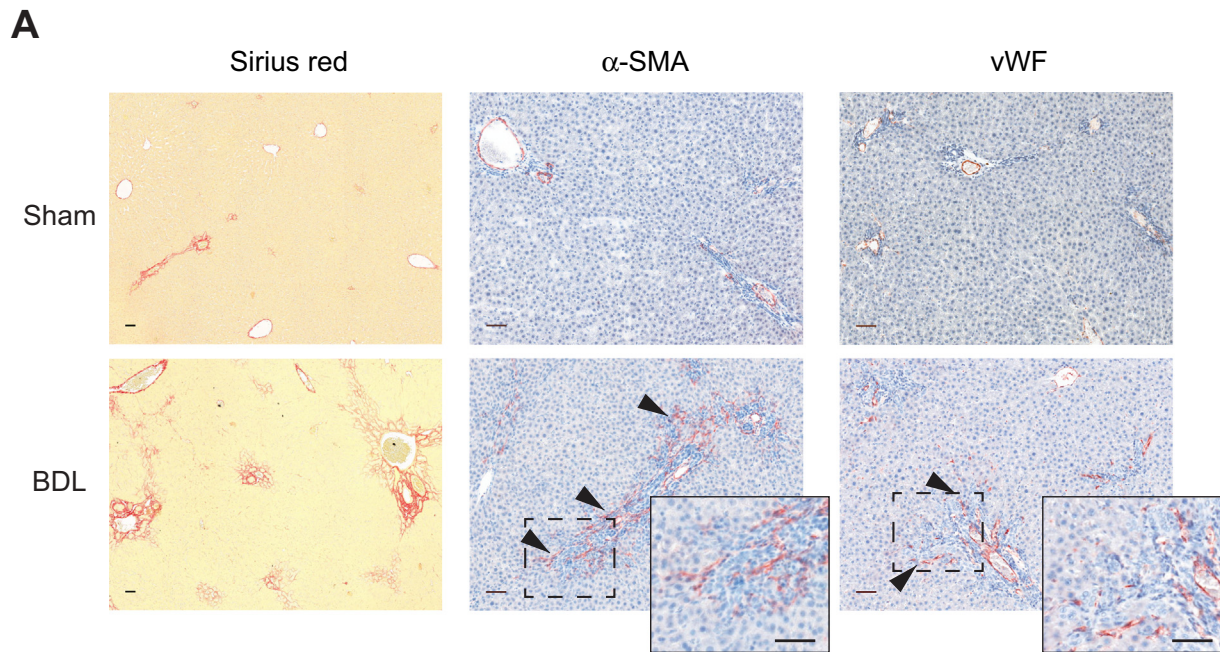
Cells were harvested in RIPA buffer with protease and phosphatase inhibitors. Proteins (30 μ g) were resolved by SDS-PAGE and transferred to nitrocellulose membranes. The following antibodies were used as primary antibodies: anti- α -SMA (#M0851; Dako), anti-GADD34 (#sc8327; Santa Cruz Biotechnology), anti-LC3I/II (#PM036; MBL International, Woburn, MA, USA), anti- α -tubulin (#T8203; Merck), anti- β -actin (#3700; Cell signaling, Danvers, MA, USA) and anti-GAPDH (#GTx627408; Clinisciences).

2.7. ELISA

ELISA was performed according to the manufacturer's instructions to measure the concentrations of collagen 1 (COL1) (#SEA571Ra, Euromedex, Souffelweyersheim, France) and vascular endothelial growth factor (VEGF) (#RRV00, R&D Systems, Minneapolis, MN, USA), in the supernatant of PMF incubated with 10% FBS-containing medium or serum-free medium, respectively, for 24 h. All samples were run in duplicate.

2.8. Cell proliferation

The proliferation of standard PMF at P1 was analyzed by two



(caption on next page)

Fig. 1. Phenotype of portal myofibroblasts (PMF) following *in vivo* expansion. (A) Liver tissue sections from bile duct-ligated (BDL) and sham-operated rats, on post-operative week 2, were subjected to Sirius red staining (original magnification $\times 10$), alpha-smooth muscle actin (α -SMA) and von Willebrand factor (vWF) immunostaining (original magnification $\times 20$); arrowheads point to stained cells at the leading or lateral edge of portal fibrosis. Insets: higher magnification of the boxed areas. Bar scale: 50 μ m. (B–G) Standard PMF (PMF) and BDL PMF derived from normal and BDL rats, respectively, were subjected to the following comparative analyses: B) RT-qPCR of *Acta2* and *Col1a1* mRNA; C) Immunoblot of α -SMA; D) ELISA of secreted collagen 1 (COL1); E) Assessment of proangiogenic activity by hemoglobin concentration in Matrigel plug assay (left panel showing representative explanted Matrigel plugs), RT-qPCR of *Vegf* mRNA (middle panel), ELISA of secreted VEGF (right panel); F) Fetal bovine serum (FBS)-induced proliferation, assessed by the percentage of Ki67-positive cells; G) FBS-induced migration, assessed by wound healing assay. Left panel showing representative phase-contrast pictures at time 0 and 24 h after insert removal; right panel showing the percentage of area covered by PMF after 24 h. Quantitative data represent means \pm SD of 5–18 cell preparations; *P < 0.05, ** P < 0.01, ***P < 0.001.

methods. Real-time cell proliferation was assessed using xCELLigence RTCA-DP System (Roche Diagnostics). By measuring electrical impedance, this device provides means to quantify cell number, viability and morphology. Cell-sensor impedance is expressed as an arbitrary unit called Cell Index. Cells were seeded in triplicate at 5000 cells/well in the E-Plate 96 (Roche Diagnostics) and allowed to grow for 24 h. After 24 h of serum deprivation, cells were incubated in DMEM with or without 10% FBS or with 50 ng/mL of fibroblast growth factor-2 (FGF2) or 100 ng/mL of monocyte chemoattractant protein-1 (MCP-1) in the presence of 0.5% FBS. Data were analyzed using RTCA Software 1.2 and expressed as means \pm SD of cell index at 24 h normalized to the cell index before stimulation.

Cell proliferation was also measured using the Click-it EdU microplate assay (Life Technologies, Paisley, UK). Briefly, cells were seeded in microplate (5000 cells/well) and after 24 h of serum deprivation, they were incubated in DMEM with or without 10% FBS in the presence of EdU for 24 h. EdU labeling was detected by fluorescence following the manufacturer's instructions.

Both aforementioned methods require cell counting before seeding, which was not possible for BDL PMF directly obtained by outgrowth at P0. Therefore, the proliferation of BDL PMF and of standard PMF to which they were compared, was assessed by Ki67 immunostaining. Cells were fixed in 4% paraformaldehyde for 15 min, then blocked and permeabilized with 2% bovine serum albumin (BSA)-0.1% Triton X100, for 1 h. Cells were then incubated with the Alexa Fluor 488-conjugated Ki67 antibody (#11882; Cell Signaling) overnight at 4 °C and nuclear staining was performed using DAPI. Ki67-positive cells were counted in five random fields at magnification $\times 20$ using ImageJ software and reported to the total number of cells.

2.9. Cell migration

Wound-healing was performed, using a culture insert made of two reservoirs separated by a 500- μ m-thick wall. An equal number of cells (25000) were plated in the two reservoirs. At confluence, cells were treated as indicated in the presence of 2 μ g/mL mitomycin-C to prevent further proliferation. The insert was removed and images were acquired between time 0 and 24 h. The area of wound coverage was calculated using the cell image analysis software ImageJ and normalized for the 0-h time point area.

Cell migration was also assessed using the xCELLigence RTCA-DP system and CIM-plates 16 (Roche Diagnostics). After 24 h of serum deprivation, cells were treated with TM (1 μ mol/L) for 24 h. Cells were seeded in the upper chamber of the CIM-plate in serum-free medium, whereas DMEM with or without FBS or with 50 ng/mL of platelet-derived growth factor-BB (PDGF-BB) was added to the lower chamber. The impedance value of each well was monitored during 24 h and data analysis was performed, using the RTCA software. Data are expressed as the rate of migration (slope) during the first 9 h.

2.10. Matrigel-plug assay

Matrigel preparations were obtained by mixing 400 μ L of growth factor-reduced Matrigel (BD Biosciences, Bedford, MA, USA) with 5 IU of heparin and 100 μ L of standard PMF or BDL PMF conditioned medium and injected subcutaneously into wild-type C57BL/6J mice

(Janvier Labs). Seven days after injection, the plugs were removed for macroscopic analysis and the hemoglobin concentration was measured using Drabkin's reagent (Sigma-Aldrich). Briefly, gel plugs were homogenized in RIPA buffer and centrifugated (8000 rpm at 4 °C, for 10 min). The supernatant was mixed with Drabkin's reagent and absorbance at 540 nm was measured. The hemoglobin concentration was calculated using a standard curve, according to the manufacturer's instructions.

2.11. Statistical analysis

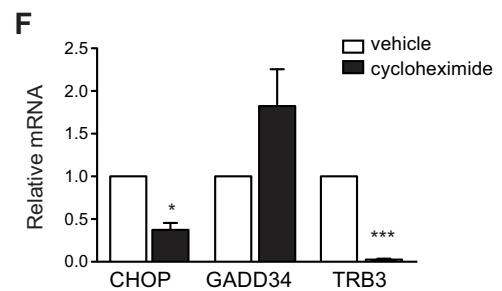
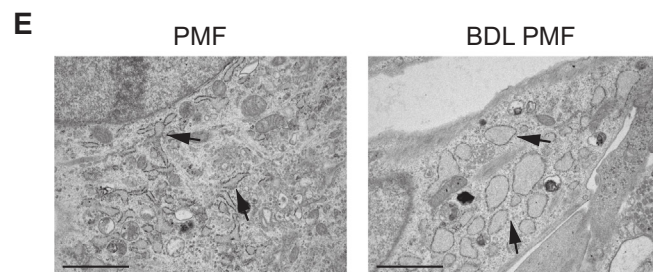
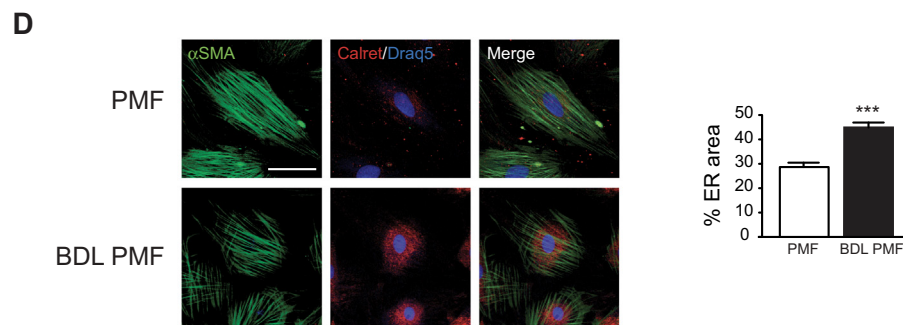
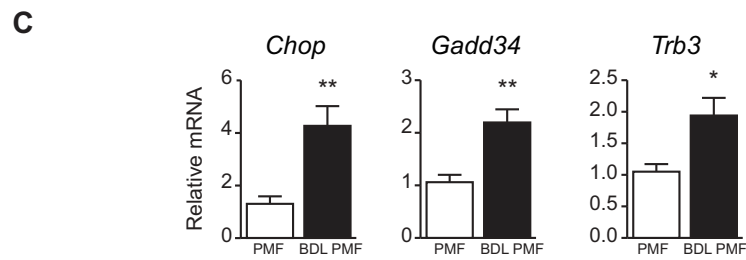
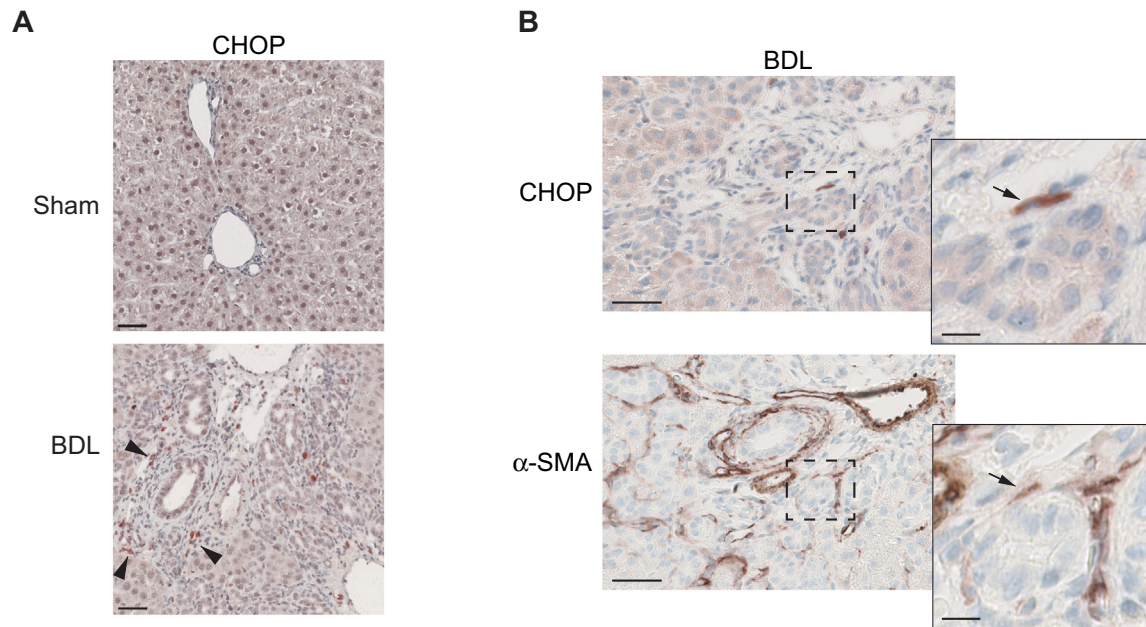
GraphPad Prism Software was used to perform statistical analysis. The Student *t*-test was used for comparisons. A P value of < 0.05 was considered significant.

3. Results

3.1. PMF expanding *in vivo* develop ER stress

PMF arise from the proliferation and myofibroblastic differentiation of portal mesenchymal progenitors in response to liver injury. They promote fibrosis and angiogenesis. In the BDL rat model, PMF accumulate around proliferating bile ducts [4]. Two weeks after BDL in rats of the present study, bile duct structures were surrounded by α -SMA-stained PMF that had migrated at the leading edge of fibrosis together with newly formed vessels (Fig. 1A). PMF that we refer to as BDL PMF, were obtained out of bile duct isolates from these BDL rats. Compared to standard PMF that emerged in culture from normal bile ducts, BDL PMF that arose *in vivo*, expressed *Acta2*/ α -SMA and *Col1a1* at higher levels and secreted larger amounts of collagen 1 (COL1) (Fig. 1, B–D), indicating that they were at a more advanced stage of myofibroblastic differentiation than standard PMF. BDL PMF were also more pro-angiogenic than standard PMF, as shown by Matrigel plug assay (Fig. 1E, left panel). To a large extent, this could be explained by a higher synthesis and secretion of VEGF (Fig. 1E, middle and right panels). By contrast, however, the proliferative and migratory capacity was lower in BDL PMF than in standard PMF, as shown in response to serum (Fig. 1, F and G). We concluded from these results that some of the fundamental functions of myofibroblasts, undergo opposite regulations in PMF following their expansion *in vivo*.

Next, we addressed the question as whether ER stress occurs and impacts phenotypic features in PMF. In the liver of BDL rats, the ER stress marker CHOP was detected by immunostaining in periductular cells consistent with PMF as shown by α -SMA staining, at the leading edge of portal fibrosis (Fig. 2, A and B). This suggested that PMF that emerged *in vivo* during BDL-induced fibrogenesis, developed ER stress, which was confirmed by the investigation of ER stress pathways in BDL PMF. Downstream targets of the PERK pathway, *i.e.* *Chop*, *Gadd34* and *Trb3*, were all overexpressed in BDL compared to standard PMF (Fig. 2C). The other two pathways of UPR, *i.e.* IRE1 and ATF6, were not activated (Supplementary Fig. S1A), suggesting a specific induction of the PERK pathway in PMF, following their expansion *in vivo*. We found no accumulation of LC3II, the conjugated form of LC3, in BDL PMF (Supplementary Fig. S1B), indicating no link with autophagy. Morphologically, the ER in BDL PMF was enlarged and dilated, as shown by calreticulin immunostaining and transmission electron microscopy



(caption on next page)

Fig. 2. Endoplasmic reticulum (ER) stress in PMF following *in vivo* expansion. (A, B) Liver tissue sections from BDL and sham-operated rats on post-operative week 2 were subjected to immunohistochemistry, showing that in BDL rats, CHOP staining is detected in periductular cells A) accumulating at the leading edge of portal fibrosis (arrowheads); B) expressing α -SMA, as shown on serial tissue sections (arrows). Original magnification $\times 20$; bar scale: 50 μ m. Insets: higher magnification of the boxed areas; bar scale: 10 μ m. (C–F) Standard PMF (PMF) and BDL PMF derived from normal and BDL rats, respectively, were subjected to the following analyses: C) RT-qPCR of *Chop*, *Gadd34* and *Trb3* mRNA; D) Co-immunostaining for α -SMA and calreticulin. Representative images (original magnification $\times 40$; bar scale: 50 μ m) are shown (left panel); ER size relative to the total cell surface, quantified by Image J (right panel); E) Transmission electron microscopy. Arrows point to ER (original magnification $\times 10000$; bar scale: 0.1 μ m); (F) RT-qPCR of *Chop*, *Gadd34* and *Trb3* mRNA in BDL PMF treated with 1 μ g/mL cycloheximide or vehicle (DMSO) for 18 h. Quantitative data represent means \pm SD of 3–13 cell preparations; *P < 0.05, ** P < 0.01, *** P < 0.001.

(Fig. 2, D and E). The overproduction of extracellular matrix components in BDL PMF compared to standard PMF likely explained these morphological features, so that protein overload could be the cause of ER stress in BDL PMF. To test this hypothesis, we treated BDL PMF with cycloheximide, a potent inhibitor of protein synthesis, which indeed reduced the expression of *Chop* and *Trb3* in these cells (Fig. 2F). This was not the case for *Gadd34* expression, which even showed a trend towards increased expression, consistent with previous data indicating that the reduction of protein synthesis by itself, is able to increase GADD34 expression [22]. Collectively, our results indicated that ER stress occurred in PMF that accumulated *in vivo* during liver fibrogenesis, likely as a result of increased secretory activity.

3.2. ER stress regulates PMF functions

To establish a potential link between ER stress and the phenotype of BDL PMF that expanded *in vivo*, we treated standard PMF obtained from normal rat liver with TM, a classical ER stress inducer. As anticipated, the treatment of PMF with TM caused a significant increase in the expression of the ER stress targets, *Chop*, *Gadd34* and *Trb3* (Fig. 3A). No change in α -SMA or *Col1a1* expression nor in COL1 secretion was observed in PMF following TM treatment (Fig. 3, B–D), indicating that ER stress had no impact on the process of myofibroblastic differentiation in these cells. We then examined the effect of TM on serum-induced proliferation and migration of PMF. TM treatment fully abolished the proliferative response (Fig. 3E) and significantly decreased the migratory response (Fig. 3F) of PMF to serum. The proliferative response of PMF to FGF2 and MCP-1 and their migratory response to PDGF-BB were also inhibited as a result of TM treatment (Supplementary Fig. S2). On the contrary, VEGF synthesis and secretion increased in PMF, following TM treatment, and *in vivo*, their proangiogenic capacity was increased, as shown by Matrigel plug assay (Fig. 3G).

3.3. PERK mediates the regulation of PMF functions by ER stress

Next, we sought to determine if PERK, the UPR pathway induced by ER stress in PMF, exerted regulatory functions in these cells. We inhibited the PERK pathway in BDL PMF using the specific inhibitor GSK2656157 [23]. The treatment of BDL PMF with 1 μ mol/L GSK2656157 reduced the expression of *Chop*, *Gadd34* and *Trb3*, the downstream targets of the PERK pathway (Fig. 4A). Such inhibition of the PERK pathway had no effect on the expression of *Acta2* or *Col1* (Fig. 4B) nor on the secretion of COL1 (Fig. 4C), confirming that ER stress had little influence on the myofibroblastic differentiation of PMF. GSK-treated BDL PMF displayed an increased proliferation rate (Fig. 4D) and migratory capacity (Fig. 4E), compared with vehicle-treated cells. By contrast, GSK treatment decreased the expression and secretion of VEGF by BDL PMF, as well as their proangiogenic activity (Fig. 4F). Together, these results indicated that the PERK pathway was induced in PMF following their expansion *in vivo* and regulated their phenotype. Whereas the proliferation and migration of PMF were down-regulated by the PERK pathway, their pro-angiogenic function was stimulated by this same pathway.

4. Discussion

In the present study, we showed that PMF develop ER stress as they expand *in vivo* during the progression of fibrosis. In its turn, ER stress, most notably the PERK pathway, further increases the proangiogenic activity of these cells, but also paradoxically inhibits their proliferation and migration.

PMF issued from the liver of BDL rats, exhibited an overexpression of the PERK downstream targets *Chop*, *Gadd34* and *Trb3*, from which we inferred that PMF developed ER stress as they accumulated *in vivo*. Of particular interest, *in situ*, CHOP was detected at the leading edge of fibrosis, where PMF accumulate [4] and where angiogenesis is the most active [24]. PMF synthesize and secrete large amounts of extracellular matrix components, which we hypothesized might trigger UPR. In keeping with this hypothesis, the global inhibition of protein synthesis by means of cycloheximide in BDL PMF, reduced ER stress. However, we cannot exclude that the pathological microenvironment, *e.g.* inflammation or hypoxia, previously shown to induce ER stress in hepatocytes, also participated in the induction of ER stress in PMF.

We found that ER stress did not contribute to the myofibroblastic phenotype of PMF. Neither the induction of ER stress by TM in standard PMF issued from normal rats nor the inhibition of the PERK pathway in *in vivo*-differentiated PMF derived from BDL rats, caused any change in the expression of α -SMA or the production of collagen. This is in contrast with what was previously observed in HSC, in which TM treatment stimulated the differentiation into myofibroblasts [15]. It was shown that ER stress stimulated the myofibroblastic differentiation of HSC by a mechanism involving the IRE1/XBP1 pathway and the activation of autophagy [17,18]. We found no activation of the IRE1 branch of UPR nor evidence of autophagy in BDL PMF, which had accumulated two weeks after the BDL trigger. However, we cannot exclude that such mechanisms took place at earlier stage of PMF differentiation following BDL-induced liver injury.

We also found that ER stress negatively regulated the proliferation and migration of PMF. Among the potential pathways mediating the anti-proliferative effect of ER stress, *Trb3*, the expression of which was increased in BDL PMF, was previously described as a negative regulator of Akt. This was shown in carcinoma cells, in which the down-regulation of *Trb3* expression caused a hyperphosphorylation of Akt and an increase in proliferation [25]. In TM-treated fibroblasts, it was also shown that PERK inhibited cyclin D1 translation, which resulted in cell-cycle arrest [26]. After they had proliferated *in vivo*, BDL PMF showed a switch towards decreased proliferative capacity, without any evidence of cellular senescence or apoptosis (not shown), even if CHOP is not only a negative regulator of cell growth but also a promoter of apoptosis [27]. Apoptosis was shown to occur as a result of TM- or cannabidiol-induced ER stress in myofibroblastic HSC [19,28]. It was also shown that ER stress contributed to the apoptosis of HSC, that takes place during the resolution of fibrosis [28]. HSC-derived myofibroblasts are intrinsically much more prone than PMF to undergo apoptosis [29], which may explain a different susceptibility to ER stress-induced apoptosis. It was suggested in a recent study that ER stress might actually cause apoptosis also in PMF, although direct evidence is currently lacking [30].

Previous work indicates that the three branches of the UPR stimulated the expression of VEGF [31,32]. In keeping with these lines, we

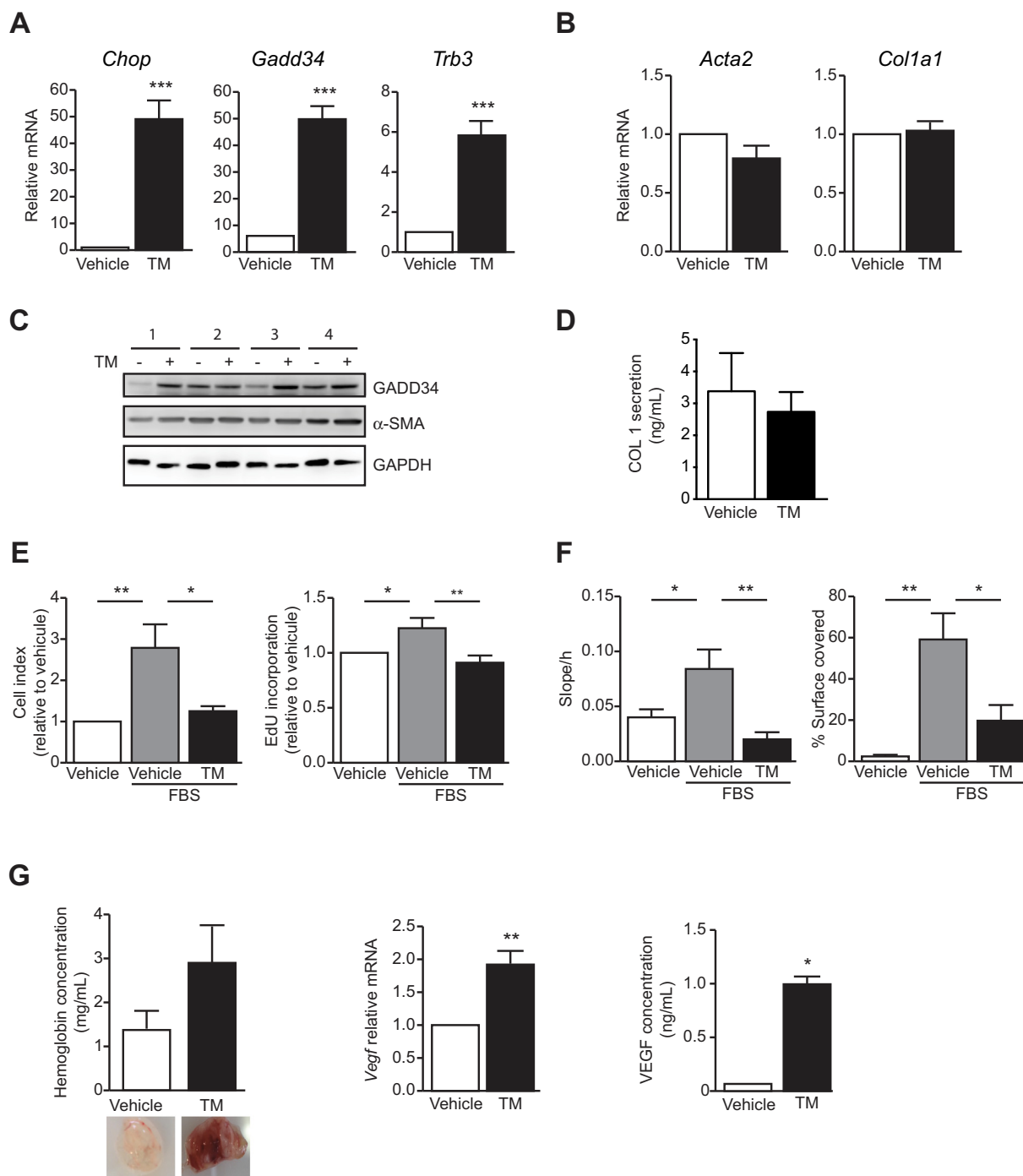


Fig. 3. Effect of tunicamycin-induced ER stress on PMF functions. Standard PMF derived from normal rats were incubated with 1 μ mol/L of tunicamycin (TM) or vehicle (DMSO) in culture and subjected to the following comparative analyses: (A) RT-qPCR of *Chop*, *Gadd34* and *Trb3* mRNA; (B) RT-qPCR of *Acta2* and *Coll1a1* mRNA; (C) Immunoblot of GADD34 and α -SMA (numbers stand for replicates); (D) ELISA of secreted collagen 1 (COL1); (E) FBS-induced proliferation, assessed by the xCELLigence System (left panel) and by EdU incorporation (right panel). Data are expressed relative to the value of vehicle-treated PMF incubated without FBS; (F) FBS-induced migration, assessed by the xCELLigence System (left panel) and by wound healing assay (right panel); (G) Proangiogenic activity assessed by hemoglobin concentration in Matrigel plug assay (left panel showing representative explanted Matrigel plugs), RT-qPCR of *Vegf* mRNA (middle panel), ELISA of secreted VEGF. Quantitative data are reported as means \pm SD of 4–16 cell preparations; *P < 0.05, ** P < 0.01, ***P < 0.005.

found that PMF undergoing ER stress displayed increased synthesis and secretion of VEGF and a high pro-angiogenic activity. We previously demonstrated that PMF signaled to endothelial cells through VEGF-laden microparticles and acted as mural cells for newly formed vessels, whereby they promoted the vascular remodeling that leads to cirrhosis [8]. By triggering the formation of scar vessels, which provide a backbone for the deposition of extracellular matrix, PMF thus appear to

be critical in the progression of fibrosis towards cirrhosis. Therefore, by increasing the pro-angiogenic activity of PMF, ER stress could also foster liver fibrosis. To address this possibility, we tested the PERK inhibitor GSK2656157 *in vivo*. In BDL rats treated with this inhibitor, we found no significant effect on fibrosis or angiogenesis (Supplementary Fig. S3), although we cannot exclude insufficient local bioavailability of the drug. Targeting PERK could also interfere with ER stress occurring

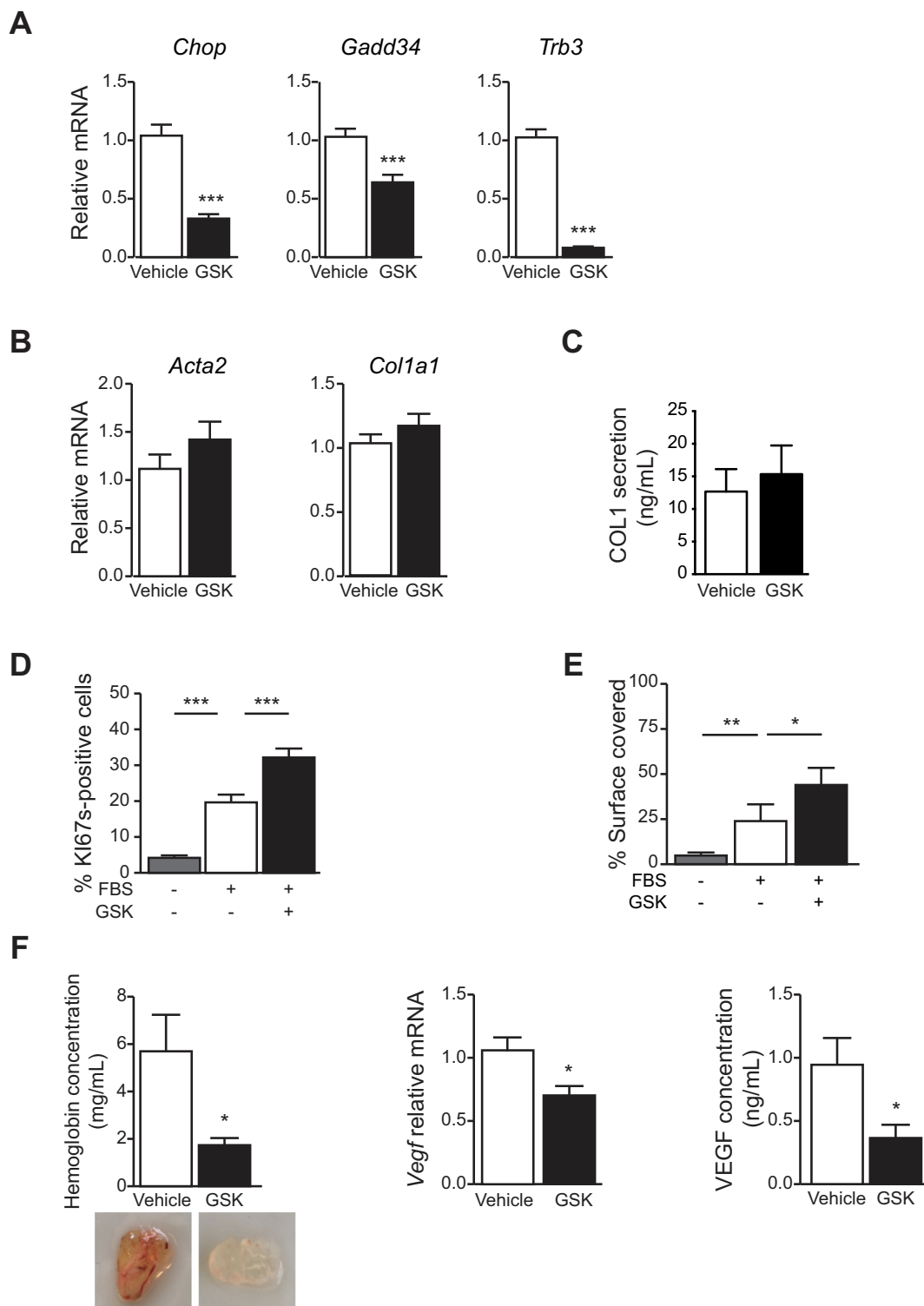


Fig. 4. Effect of PERK inhibition on the functions of *in vivo*-expanded PMF. BDL PMF derived from BDL rats were treated with 1 μmol/L GSK2656157 (GSK) or vehicle (DMSO) and subjected to the comparative analyses of (A) *Chop*, *Gadd34* and *Trb3* mRNA, (B) *Acta2* and *Col1a1* mRNA, by RT-qPCR, (C) secreted collagen 1 by ELISA (COL1); (D) FBS-induced proliferation, assessed by the percentage of Ki67-positive cells; (E) FBS-induced migration, assessed by wound healing assay; (F) Proangiogenic activity, assessed by hemoglobin concentration in Matrigel plug assay (left panel showing representative explanted Matrigel plugs), RT-qPCR of *Vegf* mRNA (middle panel), ELISA of secreted VEGF. Quantitative data are reported as means ± SD of 5–14 cell preparations; *P < 0.05, ** P < 0.01, ***P < 0.005.

outside the liver after BDL, such as in the intestine [33]. In any event, PERK does not appear as a prime target to inhibit in liver fibrosis.

To conclude, during fibrogenesis, myofibroblasts and their precursors undergo phenotypic changes, that are often described as a unidirectional process called “activation”. The current findings indicate

that this view is incorrect and that different functions of myofibroblasts can be regulated in opposite directions. After they initially expand in the injured liver as a result of active proliferation and migration, PMF become highly pro-angiogenic but less proliferative and migratory. This phenotypic switch is induced at least partly by ER stress and may

provide a mechanism that restricts the expansion of PMF as they stabilize newly formed vessels at the leading edge of fibrosis.

Supplementary data to this article can be found online at <https://doi.org/10.1016/j.bbadis.2018.10.008>.

Transparency document

The Transparency document associated with this article can be found, in online version.

Acknowledgements

The authors thank Romain Morichon and Fatiha Merabte, UMS LUMIC, for cell microscopy and histomorphology, Marie-Christine Verpont, UMR_S 1155, for electron microscopy and the PHEA team for animal care. We acknowledge Jeffrey Axten (GlaxoSmithKline, PA, USA) for providing the PERK inhibitor for *in vivo* experiments. This work was supported by funding from the Microbiome Foundation, Paris, France.

References

- [1] B. Hinz, S.H. Phan, V.J. Thannickal, M. Prunotto, A. Desmouliere, J. Varga, O. De Wever, M. Mareel, G. Gabbiani, Recent developments in myofibroblast biology: paradigms for connective tissue remodeling, *Am. J. Pathol.* 180 (2012) 1340–1355.
- [2] S.L. Friedman, Hepatic stellate cells: protean, multifunctional, and enigmatic cells of the liver, *Physiol. Rev.* 88 (2008) 125–172.
- [3] N. Kinnman, C. Francoz, V. Barbu, D. Wendum, C. Rey, R. Hultcrantz, R. Poupon, C. Housset, The myofibroblastic conversion of peribiliary fibrogenic cells distinct from hepatic stellate cells is stimulated by platelet-derived growth factor during liver fibrogenesis, *Lab. Invest.* 83 (2003) 163–173.
- [4] M. Beaussier, D. Wendum, E. Schiffer, S. Dumont, C. Rey, A. Lienhart, C. Housset, Prominent contribution of portal mesenchymal cells to liver fibrosis in ischemic and obstructive cholestatic injuries, *Lab. Invest.* 87 (2007) 292–303.
- [5] Z. Li, J.A. Dranoff, E.P. Chan, M. Uemura, J. Sevigny, R.G. Wells, Transforming growth factor-beta and substrate stiffness regulate portal fibroblast activation in culture, *Hepatology* 46 (2007) 1246–1256.
- [6] K. Iwaisako, C. Jiang, M. Zhang, M. Cong, T.J. Moore-Morris, T.J. Park, X. Liu, J. Xu, P. Wang, Y.H. Paik, F. Meng, M. Asagiri, L.A. Murray, A.F. Hofmann, T. Iida, C.K. Glass, D.A. Brenner, T. Kisseleva, Origin of myofibroblasts in the fibrotic liver in mice, *Proc. Natl. Acad. Sci. U. S. A.* 111 (2014) E3297–E3305.
- [7] I. Lua, Y. Li, J.A. Zagory, K.S. Wang, S.W. French, J. Sevigny, K. Asahina, Characterization of hepatic stellate cells, portal fibroblasts, and mesothelial cells in normal and fibrotic livers, *J. Hepatol.* 64 (2016) 1137–1146.
- [8] S. Lemoine, A. Cadoret, P.E. Rautou, H. El Mourabit, V. Ratzu, C. Corpechot, C. Rey, N. Bosselut, V. Barbu, D. Wendum, G. Feldmann, C. Boulanger, C. Henegar, C. Housset, D. Thabut, Portal myofibroblasts promote vascular remodeling underlying cirrhosis formation through the release of microparticles, *Hepatology* 61 (2015) 1041–1055.
- [9] B. Tuchweber, A. Desmouliere, M.L. Bochaton-Piallat, L. Rubbia-Brandt, G. Gabbiani, Proliferation and phenotypic modulation of portal fibroblasts in the early stages of cholestatic fibrosis in the rat, *Lab. Invest.* 74 (1996) 265–278.
- [10] J.A. Dranoff, R.G. Wells, Portal fibroblasts: underappreciated mediators of biliary fibrosis, *Hepatology* 51 (2010) 1438–1444.
- [11] H. El Mourabit, E. Loeuillard, S. Lemoine, A. Cadoret, C. Housset, Culture model of rat portal myofibroblasts, *Front. Physiol.* 7 (2016) 120.
- [12] S. Lemoine, D. Thabut, C. Housset, Portal myofibroblasts connect angiogenesis and fibrosis in liver, *Cell Tissue Res.* 365 (2016) 583–589.
- [13] L. Dara, C. Ji, N. Kaplowitz, The contribution of endoplasmic reticulum stress to liver diseases, *Hepatology* 53 (2011) 1752–1763.
- [14] P. Puri, F. Mirshahi, O. Cheung, R. Natarajan, J.W. Maher, J.M. Kellum, A.J. Sanyal, Activation and dysregulation of the unfolded protein response in nonalcoholic fatty liver disease, *Gastroenterology* 134 (2008) 568–576.
- [15] J.H. Koo, H.J. Lee, W. Kim, S.G. Kim, Endoplasmic reticulum stress in hepatic stellate cells promotes liver fibrosis via PERK-mediated degradation of HNRNP1A1 and up-regulation of SMAD2, *Gastroenterology* 150 (2016) 181–193 (e188).
- [16] N. Tamaki, E. Hatano, K. Taura, M. Tada, Y. Kodama, T. Nitta, K. Iwaisako, S. Seo, A. Nakajima, I. Ikai, S. Uemoto, CHOP deficiency attenuates cholestasis-induced liver fibrosis by reduction of hepatocyte injury, *Am. J. Physiol. Gastrointest. Liver Physiol.* 294 (2008) G498–G505.
- [17] V. Hernandez-Gea, M. Hilscher, R. Rozenfeld, M.P. Lim, N. Nieto, S. Werner, L.A. Devi, S.L. Friedman, Endoplasmic reticulum stress induces fibrogenic activity in hepatic stellate cells through autophagy, *J. Hepatol.* 59 (2013) 98–104.
- [18] R.S. Kim, D. Hasegawa, N. Goossens, T. Tsuchida, V. Athwal, X. Sun, C.L. Robinson, D. Bhattacharya, H.I. Chou, D.Y. Zhang, B.C. Fuchs, Y. Lee, Y. Hoshida, S.L. Friedman, The XBP1 arm of the unfolded protein response induces Fibrogenic activity in hepatic stellate cells through autophagy, *Sci. Rep.* 6 (2016) 39342.
- [19] M.P. Lim, L.A. Devi, R. Rozenfeld, Cannabidiol causes activated hepatic stellate cell death through a mechanism of endoplasmic reticulum stress-induced apoptosis, *Cell Death Dis.* 2 (2011) e170.
- [20] E. Borkham-Kamphorst, B.T. Steffen, E. Van de Leur, U. Haas, L. Tihaa, S.L. Friedman, R. Weiskirchen, CCN1/CYR61 overexpression in hepatic stellate cells induces ER stress-related apoptosis, *Cell. Signal.* 28 (2016) 34–42.
- [21] N. Bosselut, C. Housset, P. Marcelo, C. Rey, T. Burmester, J. Vinh, M. Vaubourdolle, A. Cadoret, B. Baudin, Distinct proteomic features of two fibrogenic liver cell populations: hepatic stellate cells and portal myofibroblasts, *Proteomics* 10 (2010) 1017–1028.
- [22] A. Dalet, R.J. Arguello, A. Combes, L. Spinelli, S. Jaeger, M. Fallet, T.P. Vu Manh, A. Mendes, J. Perego, M. Reverendo, V. Camosseto, M. Dalod, T. Weil, M.A. Santos, E. Gatti, P. Pierre, Protein synthesis inhibition and GADD34 control IFN-beta heterogeneous expression in response to dsRNA, *EMBO J.* 36 (2017) 761–782.
- [23] C. Atkins, Q. Liu, E. Minthorn, S.Y. Zhang, D.J. Figueroa, K. Moss, T.B. Stanley, B. Sanders, A. Goetz, N. Gaul, A.E. Choudhry, H. Alsaïd, B.M. Jucker, J.M. Axten, R. Kumar, Characterization of a novel PERK kinase inhibitor with antitumor and antiangiogenic activity, *Cancer Res.* 73 (2013) 1993–2002.
- [24] E. Novo, S. Cannito, E. Zamara, L. Valfre di Bonzo, A. Caligiuri, C. Cravanzola, A. Compagnone, S. Colombatto, F. Marra, M. Pinzani, M. Parola, Proangiogenic cytokines as hypoxia-dependent factors stimulating migration of human hepatic stellate cells, *Am. J. Pathol.* 170 (2007) 1942–1953.
- [25] H. Mujic, A. Nagelkerke, K.M. Rouschop, S. Chung, N. Chaudary, P.N. Span, B. Clarke, M. Milosevic, J. Sykes, R.P. Hill, M. Koritzinsky, B.G. Wouters, Hypoxic activation of the PERK/eIF2alpha arm of the unfolded protein response promotes metastasis through induction of LAMP3, *Clin. Cancer Res.* 19 (2013) 6126–6137.
- [26] J.W. Brewer, L.M. Hendershot, C.J. Sherr, J.A. Diehl, Mammalian unfolded protein response inhibits cyclin D1 translation and cell-cycle progression, *Proc. Natl. Acad. Sci. U. S. A.* 96 (1999) 8505–8510.
- [27] H. Malhi, R.J. Kaufman, Endoplasmic reticulum stress in liver disease, *J. Hepatol.* 54 (2011) 795–809.
- [28] S. De Minicis, C. Candelaresi, L. Agostinelli, S. Taffetani, S. Saccomanno, C. Rychlicki, L. Trozzi, M. Marzoni, A. Benedetti, G. Svegliati-Baroni, Endoplasmic reticulum stress induces hepatic stellate cell apoptosis and contributes to fibrosis resolution, *Liver Int.* 32 (2012) 1574–1584.
- [29] T. Knittel, D. Kobold, B. Saile, A. Grundmann, K. Neubauer, F. Piscaglia, G. Ramadori, Rat liver myofibroblasts and hepatic stellate cells: different cell populations of the fibroblast lineage with fibrogenic potential, *Gastroenterology* 117 (1999) 1205–1221.
- [30] E. Borkham-Kamphorst, B.T. Steffen, E. van de Leur, U. Haas, R. Weiskirchen, Portal myofibroblasts are sensitive to CCN-mediated endoplasmic reticulum stress-related apoptosis with potential to attenuate biliary fibrogenesis, *Cell. Signal.* 51 (2018) 72–85.
- [31] S.F. Abcouwer, P.L. Marjon, R.K. Loper, D.L. Vander Jagt, Response of VEGF expression to amino acid deprivation and inducers of endoplasmic reticulum stress, *Invest. Ophthalmol. Vis. Sci.* 43 (2002) 2791–2798.
- [32] R. Ghosh, K.L. Lipson, K.E. Sargent, A.M. Mercurio, J.S. Hunt, D. Ron, F. Urano, Transcriptional regulation of VEGF-A by the unfolded protein response pathway, *PLoS One* 5 (2010) e9575.
- [33] R. Liu, X. Li, Z. Huang, D. Zhao, B.S. Ganesh, G. Lai, W.M. Pandak, P.B. Hylemon, J.S. Bajaj, A.J. Sanyal, H. Zhou, C/EBP homologous protein-induced loss of intestinal epithelial stemness contributes to bile duct ligation-induced cholestatic liver injury in mice, *Hepatology* 67 (2018) 1441–1457.